Single shot phase shifting techniques for 4D radial slope measurements of transparent samples

N.I. Toto-Arellano
División de Óptica y Fotonica, Universidad Tecnológica de Tulancingo, Hidalgo, México,
e-mail: ivantotoarellano@hotmail.com

D.I. Serrano-García and A. Martínez García
Centro de Investigaciones en Óptica,León, Gto., México,
e-mail: david@cio.mx

G. Rodríguez-Zurita and A. Montes-Pérez
Postgrado en Óptica, Benemérita Universidad Autónoma de Puebla, Pue., México,
e- mail: gzurita@fcfm.buap.mx

J.M. Miranda-Gómez, G. Reséndiz López, A. González Rosas, and L. García-Lechuga
Área de Electromecánica Industrial, Universidad Tecnológica de Tulancingo, Hidalgo, México.

Recibido el 17 de octubre de 2011; aceptado el 18 de mayo de 2012

Through the use of non-destructive optical techniques to measure surfaces with high accuracy, a Mach-Zehnder Radial-Shear interferometer (MZRI) was implemented to analyze the radial slope of phase objects using simultaneous phase-shifting interferometry (SPSI). This optical configuration allows one to simultaneously obtain n-shearograms in order to retrieve the optical phase data map with higher accuracy. Phase reconstruction is performed using a well-known four step phase shifting algorithm. The experimental results for transparent samples are presented in this paper.

Keywords: Phase shifting; interferometry; phase grating; polarization; radial slope.

Debido a que el uso de técnicas ópticas no destructivas permite medir superficies con gran precisión, se ha implementado un interferómetro de desplazamiento radial para analizar la pendiente radial de objetos de fase usando interferometría de corrimiento de fase simultanea. Esta configuración óptica permite la obtención de n-interferogramas con desplazamiento radial simultáneamente, para recuperar el mapa de fase con mayor precisión. La reconstrucción de la fase se realiza utilizando el conocido algoritmo de cuatro corrimientos de fase. En este articulo se presentan los resultados experimentales de las muestras transparentes estudiadas.

Descriptores: Corrimiento de fase; interferometría; rejilla de fase; polarización; pendiente radial.

PACS: 42.87.Bg; 42.79.Ci; 42.79.Dj; 42.15.Eq; 42.25.Hz; 07.05.Pj

1. Introduction

Several systems have been developed to retrieve the optical phase data map in a single-capture employing polarization phase shifting techniques, this principally because of their accuracy and the effectiveness of their implementation. These systems have been employed in several fields of application, such as optical metrology [1-2], holography [3-5], optical tomography [6] and ESPI [7]. In the mentioned techniques, object information such as the refraction index, thickness or topography can be retrieved by means of the optical phase data map. Nevertheless, in some applications the measurement of the phase derivative is important [8]. In addition to that, several objects under study presents radial symmetry which makes it more convenient to use a radial shear interferometer. Because of this, we propose the use of a Radial-Shear Interferometer to properly retrieve the radial slope. Then, the main purpose of this work is to measure variations in the radial slope of transparent objects in a single capture. Experimental results for different static and dynamic transparent samples are obtained.

2. Experimental setup

Figure 1 shows the experimental setup used based on a Mach-Zehnder Radial-Shear Interferometer (MZRI) coupled to a $4f$ system. The MZRI consists of two telescope systems (S_1, S_2) [9], one on each arm, with each beam respectively presenting vertical and horizontal linear polarized light. The MZRI variants are widely used as part of different applications, so they can be considered to be representative cases of potential adaptations for simultaneous phase shifting interferometry. A $4f$ system is coupled at the end of the interferometer (dotted rectangle). This system consists of two similar achromatic lenses of focal length $f = 200$ mm and a phase grid $G(\mu, \nu)$ placed as the system's pupil with a spatial frequency $\sigma = 110$ ln/mm and a spatial period $d = 1/\sigma$. In the phase grid used, $\mu = u/\lambda f$ and $\nu = v/\lambda f$ represent the frequency along coordinates (u, v). The interferogram at the output of the MZRI consists in the interference of two versions of the same wavefront but slightly radially enlarged, and also each one with mutually orthogonal linear polarizations (vertical and horizontal). A quarter wave plate (QWP),

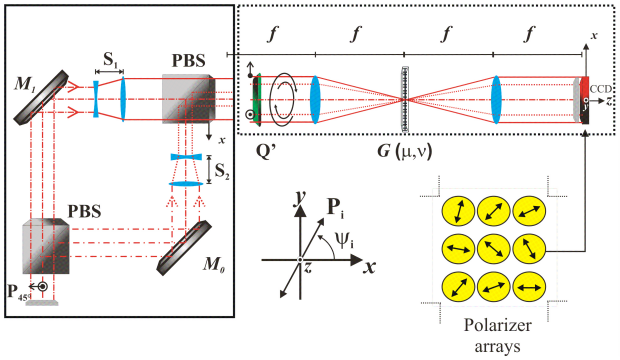

FIGURE 1. Experimental setup. Q_i:Quarter wave plate operating at 632.8 nm. $F_0 = \lambda f/d$ is the order separation. P_i: polarizing filters, ψ_i: transmission angle of polarization. PBS: Polarizing Beam splitter; M_i: Mirrors; $G(\mu,\nu)$: Phase grid. $f = 200$ mm.

Q_1 is used to obtain cross circular polarization for the radial-sheared wavefront (left and right, J_L and J_R respectively) with equal amplitudes. Replicas of the interference pattern are obtained at the output of the $4f$ system; for that reason, we placed a linearly polarized filter centered on each replica, as it is presented in Fig. 1. Cross sections of the sheared beams are $a_1 = 7.0$ mm and $a_2 = 8.6$ mm respectively, with a relative magnification of $M_a = 1.23$ [10-12]. The order separation obtained is $F_0 = \lambda f/d = 13.9216$ mm.

3. Radial slope

A transparent object without absorption is also called a phase object, and can be represented as:

$$O(x,y) = e^{i\phi(x,y)} \tag{1}$$

where $\phi(x,y)$ is taken as a real function. For a thin phase object, it is considered that $|\phi(x,y)|^2 \ll 1$, by this approximation

$$O(x,y) = 1 + i\cdot\phi(x,y) \tag{2}$$

Since the system generates two images of the same object with different radial magnifications, the interference pattern obtained has radial symmetry [9,13-14]. The interference pattern corresponds to concentric circular fringes. In this case, $r(x,y) = (x^2+y^2)^{1/2}$. From Eq. (2), the radial derivative is represented by

$$\frac{\partial O(x,y)}{\partial r(x,y)} = i\cdot\frac{\partial\phi(r(x,y))}{\partial r(x,y)} \tag{3}$$

The radial derivative of the phase object can be obtained by means of the small radial shear $\triangle r$ obtained by the interferometer; thus, we can approximate the radial change in phase with its radial derivative. The phase change introduced due to out of plane displacement (w) is given by [10-12]

$$\frac{\partial\phi(x,y)}{\partial r(x,y)} = i\cdot\frac{4\pi}{\lambda}\frac{\partial w(x,y)}{\partial r(x,y)}\triangle r \tag{4}$$

The change in the phase object associated with its radial slope is [15-16]:

$$\frac{\partial w(x,y)}{\partial r(x,y)} = C_0\frac{\partial O(x,y)}{\partial r(x,y)} \tag{5}$$

with $C_0 = i(\lambda/4\pi\Delta r)$. It can be noted that the radial derivative of the phase object is proportional to the out of plane (w) deformation, additionally maintaining a constant phase relationship of $i = \pi/2$.

4. Interference pattern replication

When the radial shear interferometer is coupled to the $4f$ system using phase grids, it is possible to obtain replicas of the interference pattern, where each one of the replicas can be separately modulated by polarization. Figure 2 shows the diffraction pattern generated by the phase grid; Figure 2(a) shows the different diffraction orders, indicated by a subscript; Figure 2(b) shows the diffraction orders generated by the grating. It can be seen that they have at least 9 diffraction orders with comparable intensities. This result is due to the modulation generated by coefficients $J_{n,l}$. Figure 2(c) shows the replicas of the interference patterns centered on each diffraction order. At the image plane, the resulting interference pattern will be the convolution of the pattern $I(x,y)$ generated at the output of the MZRI with the diffraction spectrum of the phase grid $\tilde{G}(\mu,\nu)$. Taking the contribution of one isolated term of order n,l, the irradiance obtained is proportional to [17]

$$I(x,y) = 2J_n^2J_l^2\left[1+\cos\left\{2\psi-\Delta\phi(x,y)\right\}\right] \tag{6}$$

where $\Delta\phi(x,y)$ is the phase difference, given by

$$\Delta\phi(x,y) = \phi(x/M_a, y/M_a) - \phi(x,y),$$

with M_a as the relative magnifications of the pupils. Thus, the interference patterns around a given order n,l will have orthogonal circular polarization. To detect the irradiance over each replica of the interference pattern, a linear polarized filter is placed at an angle $P(\psi)$ with respect to the horizontal axis, resulting in a phase shift $\xi = 2\psi$; as a result, an independent phase shift is obtained on each interference replica.

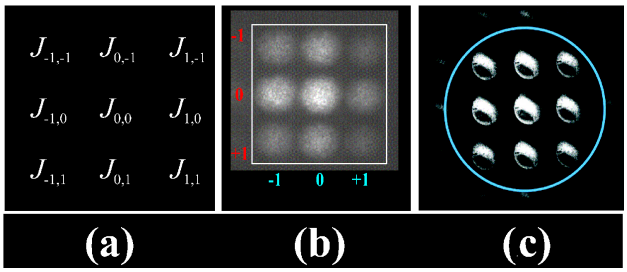

FIGURE 2. Replicas of the diffraction orders. (a) Bessel coefficients for each replica of the interference pattern. (b) Experimental diffraction orders generated by high frequency phase gratings (110 ln/mm). (c) Replicas of the interference patterns centered on each diffraction order.

5. Phase data processing

Phase reconstruction is performed using the four step phase shifting algorithm [16-20]; so, the phase can be obtained from the following equation:

$$I_i(x,y) = I_0 + M_0 \cos\left\{2\psi - \frac{\partial\phi(x,y)}{\partial r(x,y)}\Delta r(x,y)\right\} \quad (7)$$

where $I_i(x,y)$ represents the $i = 1...4$ intensity distribution captured by the CCD camera in a single shot; the angles of the polarization filters are: $\psi_1 = 0°$, $\psi_2 = 45°$, $\psi_3 = 90°$ and $\psi_4 = 135°$, and each of them represents phase shifts ξ of 0, $\pi/2$, π and $3\pi/2$ respectively. Considering that I_0 and M_0 are constant [17], the relative phase can be calculated as:

$$\frac{\partial\phi(x,y)}{\partial r(x,y)} = \arctan\left[\frac{I_1(x,y) - I_3(x,y)}{I_2(x,y) - I_4(x,y)}\right] \quad (8)$$

6. Experimental results

For the experimental results presented, we used a monochromatic camera (CMOS) with 1280×1024 pixels. Each pattern was filtered using a conventional low-pass filter to remove sharp edges and details. To reduce differences of irradiance and fringe modulation, every interferogram used was subjected to a rescaling and normalization process [21]. This procedure generates patterns of equal intensities and equal fringe modulation. However, for simplicity, the method used for unwrap the phase data was a Quality-Guided Path Following method [22]. In order to obtain the optical phase, first a reference phase map is taken to be subtracted with the phase map of the object in each capture.

The interferograms were processed using a program Called Dynamic Phase V.1 [23] using Labview 8.5. This program demodulates the fringe patterns generated by the optical system using the conventional four step phase shifting method. The four interferograms retrieved have relative $\pi/2$ phase shifts generated simultaneously and distributed in a four quadrant image. We are capable of capturing one image every 100 ms with a resolution of 480×480 pixels. The phase is obtained in quasi-real time, as the capabilities of our computer equipment do not allow images to be displayed in the monitor (the memory is saturated and images unfold slowly), so they must be stored to be later displayed frame by frame.

Figure 3 shows experimental results for samples with radial symmetry and their associated radial slopes. Figure 3(a) presents a characteristic radial shear interference pattern as a reference obtained by interfering spherical wavefronts. Figure 3(b) shows the deformed interference patterns of one drop of immersion oil placed on a microscope slide. The slope of the wavefront incident on the object is deformed by the change in phase induced by the object under study. See Fig. 3(b).

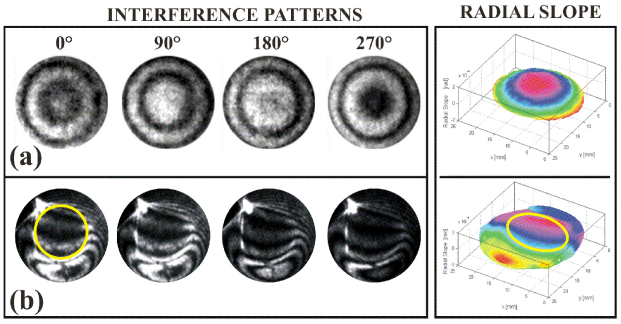

FIGURE 3. Static test objects. (a) Reference wavefront. (b) Drop of immersion oil placed on a microscope slide.

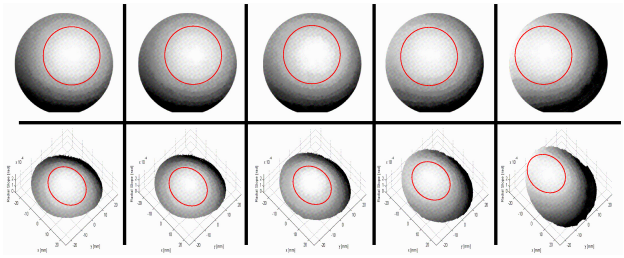

FIGURE 4. Temporal evolution of the radial slope is presented in 4D (One capture per second).

With the purpose of showing the capability of the optical system to study dynamic events [24-25], Fig. 4 presents the temporal variation of the radial slope of a misaligned lens; the misaligned lens (f=5 mm) was placed at the entrance of the MZRI, presenting the displacement of the curvature centre wavefront. As shown in the figure, when the lens moves laterally, the generated wavefront also shows a displacement; this can be clearly seen if we follow the center marked with a red circle in each phase, which moves according to the lens movement generated by the incident wavefront. This results hints at proposing this optical system as a wavefront sensor.

7. Conclusions

We have demonstrated a Mach-Zehnder Radial-Shear interferometer (MZRI) to simultaneously achieve several shearograms for slope measurements using phase-shifting techniques. The advantage of using this system is that the radial slope of the phase object is obtained in semi-real time and allows the study of transparent samples varying in time; also, this can be applied to the evaluation of wave fronts with radial symmetry.

Acknowledgements

Authors thank M. A. Ruiz for his contribution in proofreading the manuscript. Enlightening comments and references from anonymous referees are also acknowledged. Author D.-I Serrano-García (Grant: 227470/31458) is very grateful to CONACyT for the graduate scholarship granted, and expresses sincere appreciation to Geliztle. Author N.-I. Toto-

Arellano expresses sincere appreciation to Luisa, Miguel and Damian for the support provided, and to Sistema Nacional de Investigadores (SNI) for grant 47446. He currently holds a Researcher Professor position at “Universidad Tecnológica de Tulancingo” in Mexico, supporting the creation of a Photonics Engineering program at the same university.

1. J.C. Wyant, *Frontiers in Optics, OSA Technical Digest* (2004) OTuB2.
2. Y. Y. Cheng and J. C. Wyant,*Appl. Opt.* **23** (1984)4539-4543.
3. M. A. Araiza-Esquivel, L. Martínez-León, B. Javidi, P. Andrés, J. Lancis, and E. Tajahuerce, *Appl. Opt.* **50**, (2011) B96-B101.
4. I. Yamaguchi and T. Zhang, *Opt. Lett.* **22** (1997) 1268-1270.
5. T. Nomura, S. Murata, E. Nitanai, and T. Numata, *Appl. Opt.* **45** (2006) 4873-4877.
6. C. Meneses-Fabian, G. Rodriguez-Zurita, and V. Arrizón, *J. Opt. Soc. Am. A.* **23** (2006) 298-305.
7. L. C. Chen, S.-L. Yeh, A. M. Tapilouw and J.-C. Chang, *Opt. Commun.* **283** (2010) 3376-3382.
8. W. Steinchen, L. Yang, *Digital Shearography theory and Application of Digital Speckle Pattern Shearing Interferometry* (Washington, USA:SPIE Press,2003).
9. E.L. Lago and R. de la Fuente,*Appl. Opt.* **47** (2008) 372-376.
10. R.S. Sirohi, *J. Opt.* **33** (1984) 95-113.
11. P.K. Rastogi, *Digital Speckle Pattern Interferometry and Related Techniques* (Wiley 2001).
12. P.K. Rastogi, *Journal of Modern Optics* **43** (1996)1577-1581.
13. P. Hariharan and D. Sen, *J. Sci. Instrum.* **38** (1961)428-432
14. D. Malacara, *Appl. Opt.* **13** (1974) 1781-1784
15. T.W. Ng, *Opt. Commun.* **116** (1995) 31-35.
16. B. Bhaduri, N.K. Mohan, and M.P. Kothiyal,*Optics and Lasers in Eng.* **44** (2006) 637-644.
17. N.-I. Toto-Arellano *et al.*, *J. Opt.* **13** (2011) 115502.
18. B. Barrientos-García, A. J. Moore, C. Pérez-López, L. Wang and T. Tschudi, *Appl. Opt.* **38** (1999) 5944-5947.
19. B. Barrientos-García, A. J. Moore, C. Pérez-López, L. Wang and T. Tschudi, *Opt. Eng.* **38** (1999) 2069-2074.
20. D. Malacara, M. Servin, Z. Malacara, *c.6 in Phase detection algorithms in Interferogram Analysis for Optical Testing* (New York: Wiley, 2005).
21. J.A. Quiroga, J.A. Gómez-Pedrero and A. García-Botella, *Opt. Commun.* **197** (2001) 43-51.
22. C. Ghiglia and M.D. Pritt, *c.4 in Two-Dimensional Phase Unwrapping: Theory, Algorithms, and Software* (New York: John Wiley and Sons, 1998).
23. J.A. Rayas-Álvarez, N.I. Toto-Arellano, D.I. Serrano-García and A. Martinez-García, *DynamicPhase v.1*, software developed by J. A. Rayas-Álvarez *et al*, (CIO, León, Gto, México 2011).
24. N.I. Toto-Arellano, D.I. Serrano-García, A. Martínez García, G. Rodríguez Zurita and A. Montes-Pérez, *J. Opt.* **13** (2011) 115502.
25. D.-I. Serrano-García *et al.*, *Opt. Eng.* **51** 055601-1.